THE JOURNAL OF BIOLOGICAL CHEMISTRY VOL. 285, NO. 46, pp. 36049–36059, November 12, 2010

A Major Fraction of Glycosphingolipids in Model and Cellular Cholesterol-containing Membranes Is Undetectable by Their Binding Proteins*[S]

Received for publication, February 4, 2010, and in revised form, July 23, 2010 Published, JBC Papers in Press, August 17, 2010, DOI 10.1074/jbc.M110.110189

Radhia Mahfoud[‡], Adam Manis[‡§], Beth Binnington[‡], Cameron Ackerley[¶], and Clifford A. Lingwood[‡§¶‖1]

From the [‡]Division of Molecular Structure and Function, Research Institute, and the [¶]Department of Pediatric Laboratory Medicine, The Hospital for Sick Children, Ontario M5G 1X8 and the [§]Departments of Laboratory Medicine & Pathology and [‖]Biochemistry, University of Toronto, Toronto, Ontario M5S 1A8, Canada

Glycosphingolipids (GSLs) accumulate in cholesterol-enriched cell membrane domains and provide receptors for protein ligands. Lipid-based "aglycone" interactions can influence GSL carbohydrate epitope presentation. To evaluate this relationship, Verotoxin binding its receptor GSL, globotriaosyl ceramide (Gb_3), was analyzed in simple GSL/cholesterol, detergent-resistant membrane vesicles by equilibrium density gradient centrifugation. Vesicles separated into two Gb_3/cholesterol-containing populations. The lighter, minor fraction (<5% total GSL), bound VT1, VT2, IgG/IgM mAb anti-Gb_3, HIVgp120 or *Bandeiraea simplicifolia* lectin. Only IgM anti-Gb_3, more tolerant of carbohydrate modification, bound both vesicle fractions. Post-embedding cryo-immuno-EM confirmed these results. This appears to be a general GSL-cholesterol property, because similar receptor-inactive vesicles were separated for other GSL-protein ligand systems; cholera toxin (CTx)-GM1, HIVgp120-galactosyl ceramide/sulfatide. Inclusion of galactosyl or glucosyl ceramide (GalCer and GlcCer) rendered VT1-unreactive Gb_3/cholesterol vesicles, VT1-reactive. We found GalCer and GlcCer bind Gb_3, suggesting GSL-GSL interaction can counter cholesterol masking of Gb_3. The similar separation of Vero cell membrane-derived vesicles into minor "binding," and major "non-binding" fractions when probed with VT1, CTx, or anti-SSEA4 (a human GSL stem cell marker), demonstrates potential physiological relevance. Cell membrane GSL masking was cholesterol- and actin-dependent. Cholesterol depletion of Vero and HeLa cells enabled differential VT1B subunit labeling of "available" and "cholesterol-masked" plasma membrane Gb_3 pools by fluorescence microscopy. Thus, the model GSL/cholesterol vesicle studies predicted two distinct membrane GSL formats, which were demonstrated within the plasma membrane of cultured cells. Cholesterol masking of most cell membrane GSLs may impinge many GSL receptor functions.

The availability of cell membrane receptor GSL[2] carbohydrate for protein ligand binding is influenced by both the nature of the GSL lipid moiety and the membrane microenvironment (1), from early reports of membrane GSL "crypticity" (2–4) and lipid dependent anti-GSL binding (5–7), to recent fatty acid-dependent GSL bilayer remodeling (8, 9). The plane of the membrane bilayer, in relation to membrane GSLs, can markedly affect the conformation of the carbohydrate (10) to promote the availability of different epitopes within the same GSL sugar sequence (11). The local microenvironment of GSLs (membrane composition, type of solid phase support) can affect carbohydrate presentation for ligand binding (12–14). Protein binding can be regulated by the GSL fatty acid/ceramide content (15–19). Different protein ligands, which recognize the same receptor GSL, can bind differentially in a cell or model membrane context, and cholesterol can play a central role (20, 21). Cholesterol is key to the structural maintenance of membranes and interacts strongly with sphingolipids (22). This, combined with the hydrogen bond network between membrane GSLs (23), provides a (thermodynamically strained (1)) "interface" between the hydrophilic carbohydrate head group and the hydrophobic hydrocarbon tail, which can regulate GSL receptor activity (24). This is particularly relevant in the context of cellular GSL accumulation in cholesterol-enriched detergent-resistant membranes (DRMs) (25). Although the nature of DRM correlation to lipid rafts of model systems (26) is a matter of debate, detergent insolubility can be indicative of specific lateral interactions involving both lipids and proteins (27). In this context, we have found detergent resistance to be a useful probe of "aglycone" regulation of GSL receptor presentation in tissues (28, 29).

Escherichia coli-derived Verotoxins (VTs) are associated with hemolytic uremic syndrome and hemorrhagic colitis. Verotoxin 1 (VT1) and Verotoxin 2 (VT2, more frequently associated with human disease), bind the neutral GSL, globotri-

* This work was supported by CIHR Grant MT 13747, grants from Ontario HIV Treatment Network and Canfar and by the Research Training Centre at the Research Institute, Hospital for Sick Children.

[S] The on-line version of this article (available at http://www.jbc.org) contains supplemental Fig. 1 and Table 1.

[1] To whom correspondence should be addressed: Molecular Structure and Function, Research Institute, The Hospital for Sick Children, Ontario M5G 1X8, Canada. Tel.: 416-813-5998; Fax: 416-813-5993; E-mail: cling@sickkids.ca.

[2] The abbreviations used are: GSL, glycosphingolipid; Gb_3, globotriaosylceramide, galactose α1–4 galactose β1–4 glucosylceramide; Gb_4, globotetraosyl ceramide; GalCer, galactosyl ceramide; GlcCer, glucosyl ceramide; LacCer, lactosyl ceramide; SGC, sulfogalactosylceramide; Chol, cholesterol; GM1, monosialogangliotetraosyl ceramide; SSEA-4, stage-specific embryonic antigen-4 (NeuAcα2–3Galβ1–3GalNAcβ1–3Galα1–4 Galβ1–4 Glc ceramide); VT, Verotoxin; CTx, cholera toxin; CTxB, cholera toxin B-subunit; DRM, detergent-resistant membrane; MβCD, methyl β-cyclodextrin; P4, threo-1-phenyl-2-hexadecanoylamino-3-pyrrolidino-1-propanol; IEM, immuno-EM; MES, 4-morpholineethanesulfonic acid.

aosyl ceramide (Gb_3, CD77, or p^k blood group antigen) (30), but binding is affected by the lipid (aglycone) moiety (13, 17). Although VT1 and VT2 only bind Gb_3 (31), they recognize different molecular Gb_3 assemblies in the plasma membrane, which are then differentially sorted intracellularly (21). This implies cellular recognition of aglycone GSL modulation also. DRM Gb_3 is required for VT1 transmembrane signaling (32) and intracellular VT retrograde trafficking and cytotoxicity *in vitro* (33, 34) and potentially, *in vivo* (28).

Several GSLs (35), including Gb_3 (36), are bound by the HIV adhesin, gp120. Like VT, gp120/GSL binding is modulated by the lipid moiety (37). Cholesterol is important in HIV infection (38, 39), and Gb_3, and Gb_3 analogues, are HIV inhibitors (40, 41).

Elucidation of aglycone properties influencing membrane GSL carbohydrate presentation presents an experimental challenge. We developed a method to prepare simple, sucrose gradient separated, detergent-resistant GSL/cholesterol vesicles (42) with the aim of defining potential membrane components influencing GSL carbohydrate-protein ligand binding. We now find that vesicle separation has yet to equilibrate under these conditions. Prolonged centrifugation and increased gradient resolution, unexpectedly, showed ligand binding is restricted to a minor buoyant vesicle fraction, and the bulk GSL/cholesterol DRM bilayer vesicles are, in some way, unavailable for recognition. This effect was found for the binding of all GSLs tested, to their appropriate protein ligands. Surprisingly, these model vesicles proved an accurate predictor of the properties of cell-derived DRM vesicles and membrane GSL expression in cells. A large fraction of cellular GSL can be "cloaked" by cholesterol to prevent ligand recognition.

EXPERIMENTAL PROCEDURES

Materials—VT1 and VT2 were purified as described previously (43). mAb anti-VT1 (clone PH1; IgG_1) and rabbit antiserum against the VT1 B-subunit were prepared in our laboratory. Rabbit antiserum against the VT2 variant, VT2e, was a gift from Dr. C. Gyles, University of Guelph, and was used for VT2 detection. Gb_3 was purified from human kidney (44). HRP-conjugated goat anti-rabbit or mouse IgG was purchased from Bio-Rad. Monosialoganglioside (GM1), sulfatide (SGC), cholesterol, methyl β-cyclodextrin (MβCD), and latrunculin B were from Sigma. HRP-cholera toxin (CTx) B-subunit was from List Biological Labs, [^{3}H]cholesterol was from ICN. R5 HIV gp120 (a single ~120-kDa peak by gel filtration) and mAb anti-gp120 (clone F425 B4a1; IgG1) were from the NIH AIDS Research and Reference Reagent program. Rabbit anti-caveolin1 (N20) was from Santa Cruz Biotechnology (Santa Cruz, CA). Rabbit polyclonal anti-GM1 was a gift from Dr. D. Mahuran, Hospital for Sick Children Toronto. Rat IgM mAb anti-Gb_3 (clone 38.13) (45) was kindly supplied by Dr. J. Wiels, Institut Gustave Roussy, Paris. Mouse mAb anti-SSEA4 was kindly provided by Dr. R. Kannagi, Aichi Cancer Center, Nagoya, Japan. Mouse IgG_{2b} mAb anti-Gb_3 (clone BGR23) was from Seikagaku Corp. Biotinylated *Bandeiraea simplicifolia* lectin 1 was from Vector Laboratories. The glucosylceramide synthase inhibitor threo-1-phenyl-2-hexadecanoylamino-3-pyrrolidino-1-propanol (P4) (46) was purchased from Matreya and diluted from 2 mM stock solution in DMSO.

Labeling of Verotoxin—VT1 and VT2 (100–200 μg) were iodinated for 1 min with 0.2 mCi of $Na^{125}I$ (Amersham Biosciences) in an Iodogen-coated glass tube. Unreacted iodine was removed by gel-filtration chromatography using Sephadex G-25, and the specific activity (cpm/μg) was determined by protein assay. Radiolabeled VT was stored at 4 °C in PBS containing 0.5 mg/ml BSA. Radiolabeled VT exhibited no significant loss in Vero cell cytotoxicity, and binding to Vero cell monolayers was saturable and inhibited by a 10-fold excess of unlabeled toxin.

GSL/Cholesterol Vesicle Construction—GSL/cholesterol vesicles were generated by a scale reduction of the described procedure (42). Briefly, a 2:1 ratio of Gb_3 (or in some cases for gp120 binding, GalCer or sulfatide (SGC), or cholera toxin binding GM1 (50 μg) and cholesterol (25 μg) in ethanol were dried together (in later unmasking studies another GSL (50 μg) was included) and dissolved in 750 μl of MES-Triton buffer (25 mM MES, 150 mM NaCl, pH 7.2, 1% (w/v) Triton X-100). The solution was vortexed (1 min), sonicated (1 min), heated at 55 °C (5 min), and vortexed again (1 min). Then 750 μl of 70% (w/v) sucrose solution in MES buffer was added, gently mixed, and allowed to stand at room temperature for ~1 h. The mixture was placed below 1 ml of 30% sucrose containing 1 μg/ml ^{125}I-labeled VT or unlabeled VT1, VT2, mAb anti-Gb_3, gp120, or HRP-CTB, each used at 1–4 μg/ml. This was overlaid successively with 1 ml of 30% sucrose (in later experiments 25% sucrose was used to minimize mixing of this layer with the ligand-containing layer) and 1.5 ml of 5% of sucrose. Condensed lipid species were separated by flotation ultracentrifugation using an SW55Ti rotor at 34,000 rpm for 72 h, 20 °C. The duration of centrifugation was empirically defined for resolution of the GSL-bound ligand. Vesicle separation was not affected by temperature (4 °C or 20 °C) but was improved as compared with the original full scale method (42). From the top of the tube, 10 fractions, 500 μl each, were then collected and counted in a γ-counter to determine ^{125}I-VT distribution in the gradient. Unlabeled ligands were detected by dot blot as described below. In some experiments GSL/cholesterol vesicles were separated by sucrose gradient ultracentrifugation without ligand. Vesicle fraction aliquots were immobilized on nitrocellulose, and then ligand binding to the immobilized vesicles was immunodetected. In some cases fractions 9/10 were pooled.

Immunoblot Analysis of Vesicle Fractions—Equal volumes of the gradient fractions were loaded onto nitrocellulose (Whatman Protran BA85) using a dot blot apparatus (Shliecher & Schuell, Minifold I microsample filtration manifold). The samples were washed with TBS (50 mM Tris-HCl, pH 7.2, 150 mM NaCl) containing 1% skim milk or BSA blocking solution for 1 h. The membrane was rinsed with TBS and then probed for bound ligand or when ligand was not included in the gradient, used for ligand binding to the immobilized vesicles. Briefly, the immobilized vesicles were incubated with VT1, VT2, gp120, or anti-Gb_3 (1 μg/ml) for 1 h at room temperature, the blots washed, and bound ligand was detected with appropriate antibody followed by HRP-conjugated second antibody.

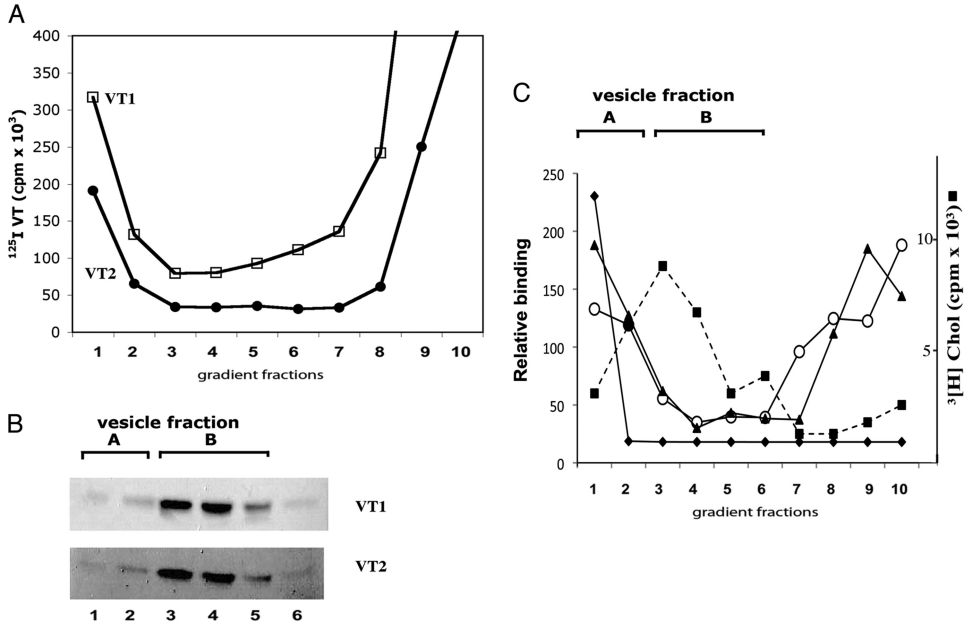

FIGURE 1. **Gb_3/cholesterol vesicles can be separated into minor VT1/VT2-binding and major non-binding fractions.** *A*, ^{125}I-VT1 (□) and ^{125}I-VT2 (●), added to vesicles before gradient centrifugation. *B*, Gb_3 in gradient fractions was extracted and detected by VT1/VT2-TLC overlay. *C*, densitometry of immunodetected exogenous VT1 (♦) or VT2 (▲) binding to gradient-separated Gb_3/cholesterol vesicle, VT1 distribution (○) in gradient fractions when added before separation. The distribution of [^{3}H]cholesterol (■) is shown.

As an alternative to determine the distribution of VT1 in gradient fractions, equal volumes from each fraction were mixed with 1/5 volume of non-reducing 5× SDS-PAGE sample buffer and heated to 90 °C for 5 min. Ten μl of each sample were subject to 15% SDS-PAGE followed by Western blotting. The VT1-A subunit was detected with rabbit polyclonal antiserum raised against the A-subunit (47). Immunoblots and TLCs were quantitated using ImageJ (48).

Post-embedding Immuno-EM of Vesicles—Gb_3/cholesterol vesicles were prepared as above and processed for post-embedding cryo-immuno-EM, either before or after separation by sucrose density centrifugation. To aid in sectioning, the vesicles were stained with toluene blue dye for 1 min before excess MES buffer was added, and the solution was vortexed and centrifuged at 20,000 rpm for 30 min at 20 °C. The pelleted vesicles were then air-dried for at least 1 h at room temperature. Vesicles were infiltrated in gelatin (20% in PBS) before cryo-freezing. Thin sections were cut using a Leica cryomicrotome and mounted on grids at the Advanced Bioimaging Centre, Hospital for Sick Children. For immunogold labeling, section grids were first washed by flotation on a drop of PBS. Sections were blocked with 1% BSA in PBS and then incubated with 5 μg/ml VT-1 in PBS followed by washing and incubation with rabbit anti-VT1 B serum diluted 1:200 in PBS (both 1 h). Bound antibodies were detected with 10 (5) nm gold-conjugated protein A. Sections were post-fixed in 2% uranyl acetate in water for 15 min at room temperature before treatment with methyl cellulose. VT1 was omitted in control sections. Sections of sucrose gradient separated "fraction B" Gb_3/cholesterol vesicles were treated with rat IgM mAb anti-Gb_3 (1 μg/ml) for 1 h, washed, and bound antibody detected with 3 nm gold-labeled goat anti-rat IgM antibody. Monoclonal rat IgM (clone eBRM) served as an isotype control to define background antibody binding to the vesicles. All steps were performed at room temperature. Stained grids were imaged using a JEM2001 transmission electron microscope.

Lipid Extraction—Lipids were extracted from sucrose fractions by one of two methods. Neutral lipids/glycolipids were isolated by extracting 150 μl of each fraction with chloroform/methanol 2:1 followed by Folch partition (49). The upper phase was removed, and the lower phase was washed 2× with theoretical upper phase to remove sucrose. The lower phase was dried under nitrogen gas, and ~25% of the sample was separated by TLC in chloroform:methanol:water 65:25:4 (v/v). Phospholipids were detected using iodine vapor and imaged by scanning prior to Gb_3 detection by VT1 overlay. Cholesterol was detected by ferric chloride spray (50). For total lipid extraction (gangliosides included), 150 μl of each fraction was mixed with an equal volume of 50% methanol in water to dissolve the membranes. The samples were loaded onto 50-mg C18 columns equilibrated in 10% aqueous methanol. Columns were washed with 50% methanol, then lipids were eluted with 2 ml of 100% methanol followed by 2 ml of chloroform:methanol (1:1). Solvent was dried, and lipids were separated using the TLC solvent chloroform:methanol:water (60:35:8). After phospholipid detection, TLC plates were probed for GM1 using biotinylated CTx B subunit and Gb_3 using VT1 (51).

Preparation of Vero Cell Membranes—Cells were grown to near confluence in four 150-cm^2 dishes, washed briefly, and harvested by scraping in 5 mM EDTA in PBS, and centrifugation at 4 °C. Glycosphingolipid-depleted cells were prepared by culture for 7 days in 2 μM P4 prior to harvest. The cells were suspended in 2 ml of 10 mM Tris-HCl, pH 7.4, 10 mM NaCl containing a protease inhibitor mixture (4-(2-aminoethyl)benzenesulfonylfluoride hydrochloride, E64, aprotinin, leupeptin, and bestatin) and disrupted by 30 strokes in a Dounce homogenizer with a tight-fitting pestle. Nuclei and debris were removed by spinning at 800 × *g* for 10 min at 4 °C. The supernatant was centrifuged at 100,000 × *g* in an SW55Ti rotor for 30 min at 4 °C. The resulting membrane pellet was suspended gently in 1 ml of ice-cold 25 mM MES, pH 7.0, 140 mM NaCl. Protein was determined using the bicinchoninic acid method (BCA assay, Pierce). Membranes stored frozen at −80 °C before use or prepared from cell pellets frozen for up to 1 month gave identical results.

For generation of DRMs, membrane preparation equivalent to 600 μg of protein was made up to a volume of 375 μl and mixed with an equal volume of 0.5% Triton X-100 on ice. The membranes were treated for 30 min on ice and equilibrated to room temperature. The sample was mixed with an equal vol-

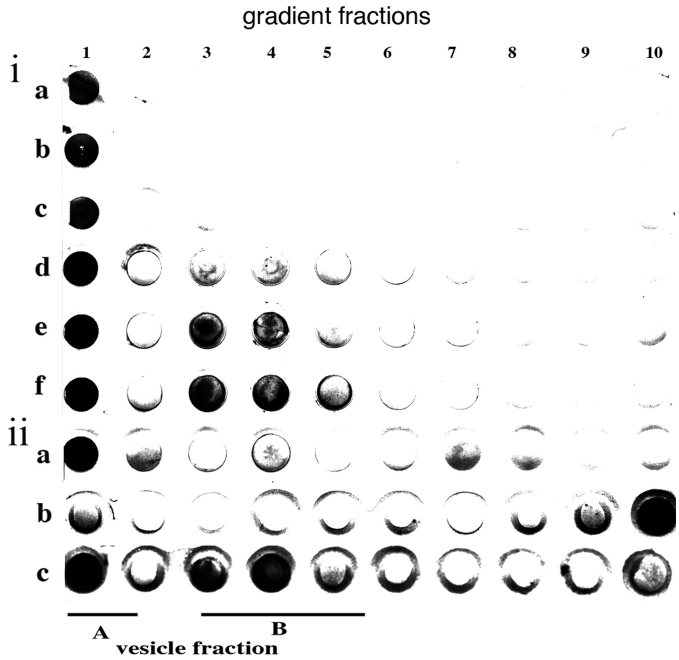

FIGURE 2. **Other Gb_3-binding proteins show a similar vesicle binding profile.** The mouse IgG mAb anti-Gb_3 (clone BGR23) was compared with the rat IgM mAb anti-Gb_3 (clone 38.13) and *B. simplicifolia* for binding sucrose gradient-separated Gb_3/cholesterol vesicles. *Panel i*: *lanes a–c* and *d–f*, increasing aliquots of the gradient-separated Gb_3 vesicles stained with the BGR23 and 38.13, respectively. *Panel ii*: binding of VT1 (*lane a*), *B. simplicifolia* lectin (*lane b*), and 38.13 (*lane c*) to sucrose gradient-separated Gb_3/cholesterol vesicles.

ume of 70% sucrose in MES buffer and allowed to sit for 1 h at room temperature, and then sucrose gradient conditions were as described for glycolipid-cholesterol mixtures. For MβCD treatment of membranes, 600 μg of membrane protein was treated with 70% sucrose containing 10 mM MβCD at room temperature for 1 h following detergent extraction and prior to sucrose gradient centrifugation. Culture cells were depleted of cholesterol by treatment with 10 mM MβCD for 10 min at 37 °C in serum-free medium.

Gb_3-GSL Binding—A partial survey of the potential of Gb_3 to bind to other GSLs and lipids was performed using a simple TLC overlay procedure we developed. 1 μg of lipid samples was applied to triplicate TLC grids and air-dried. Lipids on one grid were visualized with orcinol spray. The other two grids were blocked in TBS containing 1% BSA then washed. In a glass tube, 20 μg of Gb_3 (dried from ethanol under N_2) was suspended in 2.5 ml of TBS containing 1% BSA by heating at 40 °C for 20 min, mixed in a bath sonicator for 1 min, and gently vortexed for 30 s. The TLC grids were incubated in "aqueous Gb_3" (~8 μM Gb_3) or TBS/BSA alone for 1 h at room temperature. The grids were washed 3× with TBS, and then Gb_3 was detected by VT1 binding as described above.

Fluorescence Microscopy—Prior to labeling, cells were washed with serum-free medium (HMEM: 20 mM HEPES-buffered Erhles minimal essential medium containing 0.02% BSA) and chilled on ice. Alexa488-VT1B (5 μg/ml) was added for 20 min on ice. The cells were washed twice with HMEM then fixed, for surface labeling, or pre-warmed HMEM was added, and the cells were maintained at 37 °C for 15 min to internalize bound VT1B. The medium was replaced with HMEM (control) or

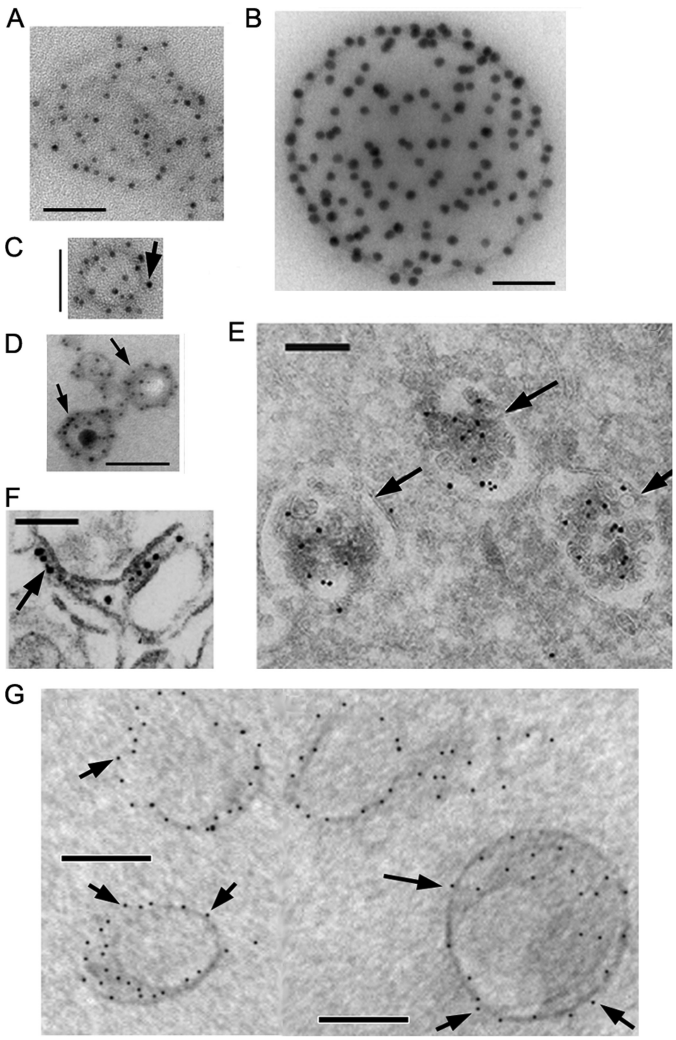

FIGURE 3. **Post-embedding cryo-immuno-EM of Gb_3/cholesterol vesicles confirms VT1 vesicle binding profile.** VT1 immunogold labeling of unfractionated Gb_3/cholesterol vesicles (*A–D*), sucrose gradient vesicle fraction A (*F*), and vesicle fraction B (*E*). IgM mAb anti-Gb_3 labeling of vesicle fraction B is in *panel G*. Because the VT1-antibody-gold or IgM anti-Gb_3-gold complex is at least 50 Å, surface binding is conclusive only when gold is external to the vesicle limiting membrane. In unseparated samples, larger vesicles (*A* and *B*) are VT1-labeled internally only, whereas VT1 labels the both bilayer leaflets of smaller vesicles (*C* and *D*, *arrows*). Inner membrane VT1 labeling of gradient separated vesicle fraction B is seen, whereas the outer membrane (*E*, *arrows*) is unlabeled. The smaller vesicles found in fraction A show outer membrane VT1 labeling (*F*, *arrow*). Rat IgM anti-Gb_3 outer membrane labeling of vesicle fraction B is shown in *G* (*arrows*). *Bar* = 100 nm. Controls in which VT1 was omitted or rat IgM isotype control used showed no labeling.

HMEM containing 10 mM MβCD for 10 min at 37 °C. Coverslips were washed twice with warm HMEM then cooled on ice. Unmasked surface Gb_3 was labeled with Texas Red-labeled VT1B (5 μg/ml) for 20 min on ice. After washing, cells were fixed on ice with 4% paraformaldehyde in PBS, washed, and then mounted in Prolong Antifade (Molecular Probes). 5 μg/ml DAPI was included in the mounting medium for nuclear labeling. Images were obtained using a Zeiss Axioplan epifluorescence microscope (21).

RESULTS

VT1 Binding to Gradient Separated Gb_3/Cholesterol Vesicles Reveals a Major Discrepancy in GSL Receptor Function—Using our method to generate detergent-resisting Gb_3/cho-

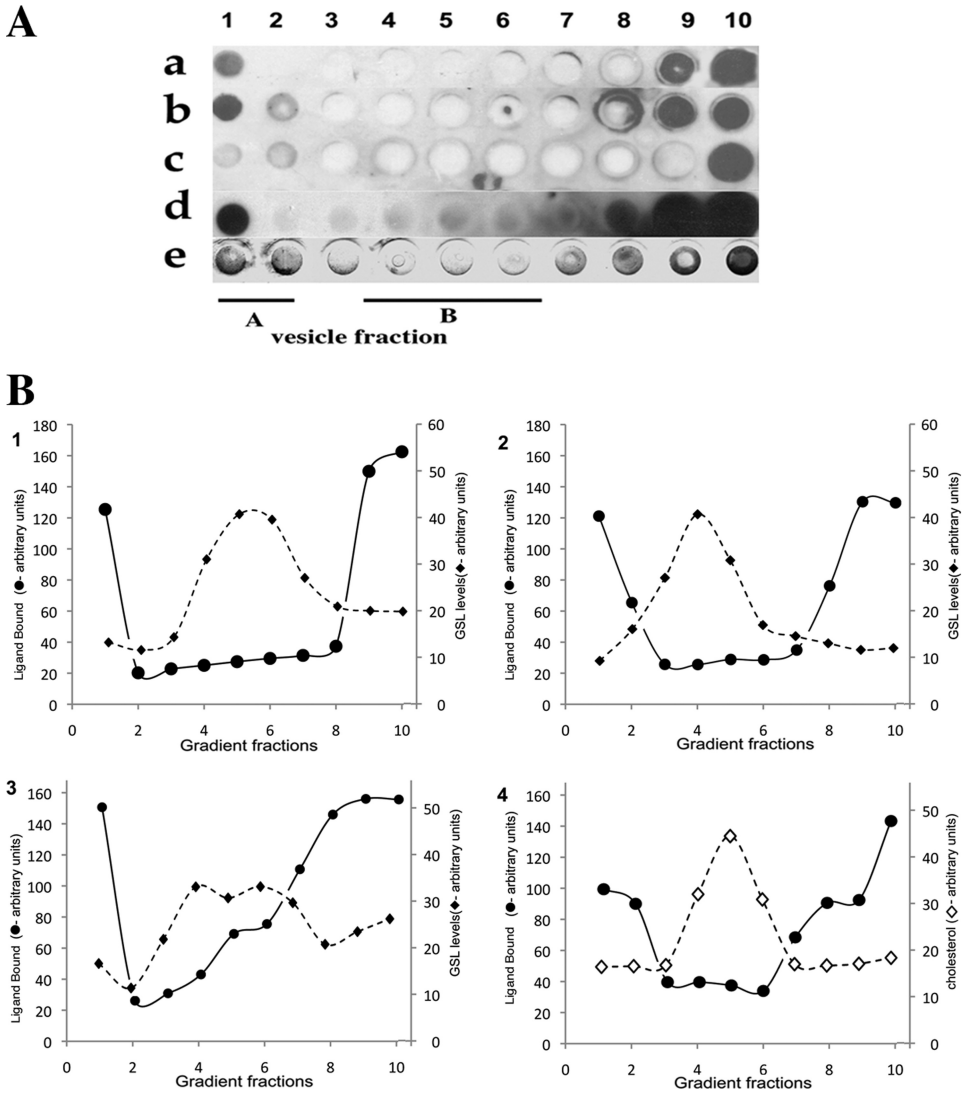

FIGURE 4. **R5 HIV-1 gp120 binding is similarly restricted to a minor fraction of GSL/cholesterol vesicles.** GSL/cholesterol vesicles were mixed with gp120, separated by sucrose gradient, and immobilized on nitrocellulose for bound gp120 immunodetection. *A*, gp120 binding to Gb_3 (*a*), GalCer (*b*), Gb_4 (*c*), and SGC gradient fractions (*d*); *e*, VT1 binding to Gb_3 sucrose gradient-separated vesicles. *B*, ligand-GSL binding in *A* was compared by densitometry (●) to gradient fraction GSL content (◆). GSLs were extracted, separated by TLC, and quantitated by densitometry of the orcinol stain. *1*, gp120 and Gb_3; *2*, gp120 and GalCer; *3*, gp120 and SGC; *4*, VT1 binding Gb_3 (●) compared with cholesterol (◇) distribution by $FeCl_3$ detection after TLC.

lesterol vesicles (42), and centrifuging to equilibrium, VT binding vesicles were separated from the bulk Gb_3 vesicles (Fig. 1). ^{125}I-VT1/VT2 bound only in the first (± second) fraction (vesicle fraction A) (Fig. 1*A*), which contained low Gb_3 levels (Fig. 1*B*). >95% of the Gb_3 was in higher density fractions (3,4,5-vesicle fraction B), not bound by VT1 or VT2. Thus, Verotoxin only binds a minor, more buoyant subset of Gb_3/cholesterol vesicles.

The cholesterol and Gb_3 gradient distributions coincide (Fig. 1, *B* and *C*). The Gb_3/cholesterol ratio, measured with [^{3}H]cholesterol, was constant at ~1.4, which approximates the micelle-to-vesicle transition for GM1/cholesterol mixtures (52). Triton was distributed throughout the gradient (not shown). Gb_3 distribution was unaffected by the presence of VT: the same result was obtained when VT1 was omitted from the gradient and post-bound to the vesicles immobilized on nitrocellulose after separation (Fig. 1*B*). In either case, only a minor subfraction (<5%) of Gb_3 vesicles at the gradient top was bound.

Other Gb_3 Ligands Only Bind the Minor Gb_3 Vesicle Fraction—An IgG mAb anti-Gb_3 showed the same restricted binding as VT1/VT2 (Fig. 2*i*, *rows a–c*). However, for an IgM mAb anti-Gb_3 (45), though vesicle fraction A remained the primary binding fraction, vesicle fraction B, the major Gb_3 fraction, was also bound (Fig. 2*i*, *rows d–f*). *B. simplicifolia* lectin, which binds the terminal α-galactose of Gb_3, was also restricted to vesicle fraction A (Fig. 2*ii*, *row b*).

Post-embedding VT1 Immuno-EM of fraction A and B Gb_3/Cholesterol Vesicles—Cryo-immuno-EM showed the Gb_3/cholesterol vesicle preparation largely comprises two sizes. VT1 bound outer (and inner) membranes of the smaller vesicles (Fig. 3, *C* and *D*) but only inner membranes of the larger vesicles (Fig. 3, *A* and *B*). After separation, fraction B contained only larger, multivesicular vesicles. VT1 binding was restricted within these vesicles (Fig. 3*E*). Gb_3 in the outer bilayer leaflet was not recognized. In contrast, the fraction A vesicles were smaller and showed outer membrane VT1 binding (Fig. 3*F*). This suggested the gradient separates the two major vesicle formats found in the starting preparation. For fraction B vesicles, stained with rat IgM anti-Gb_3, binding to both leaflets of the outer membrane was observed (Fig. 3*G*), unlike VT1 (Fig. 3*E*).

HIV gp120 Binding to GSL Vesicles Mimics That of VT1 and VT2—The HIV adhesin gp120 binds several GSLs, including Gb_3 (53). As for VT1/VT2, R5 gp120 included within the gradient only bound to Gb_3 vesicle fraction A (Fig. 4*A*, *row a*). Gp120 binds galactosyl ceramide (GalCer) and 3′-sulfogalactosyl ceramide (SGC) (35). GalCer/cholesterol and SGC/cholesterol vesicles were similarly prepared and separated in a gp120-containing density gradient. Gp120, localized by immunoblot, only bound vesicle fraction A of the separated GalCer or SGC vesicles (Fig. 4*A*, *rows b* and *d*). Vesicle fraction A had low GSL content. No gp120 binding in vesicle fraction A from a gradient of Gb_4/cholesterol vesicles was found (Fig. 4*A*, *row c*), consistent with the lack of gp120-Gb_4 recognition (36). Cholesterol (Fig. 4*B*, *graph 4*), and the majority of the GSL (*graphs 1–3*), accumulated in vesicle fraction B. No significant VT1/VT2 or gp120 binding in these fractions was detected (Fig. 4*A*).

Cholera Toxin Binds a Minor GM1/Cholesterol Vesicle Fraction—CTx-binding GM1 is a major tool in cell and model membrane studies (25). GM1/cholesterol vesicles were placed below a sucrose gradient containing CTxB-HRP. After centrifugation, fractions were stained with peroxidase substrate. CTxB was bound only in vesicle fraction A (Fig. 5, *panel 1*). By CTxB TLC overlay of lipid extracts, GM1 was concentrated in vesicle fraction B (Fig. 5, *panel 2*), as seen for Gb_3, GalCer, and SGC. Thus CTxB receptor function within GM1/cholesterol vesicles is also restricted to a minor GM1 subfraction. This was verified using a polyclonal rabbit anti-GM1 within a similar GM1/cholesterol sucrose gradient. After separation, bound antibody was only immunodetected in vesicle fraction A (Fig. 5, *panel 3*).

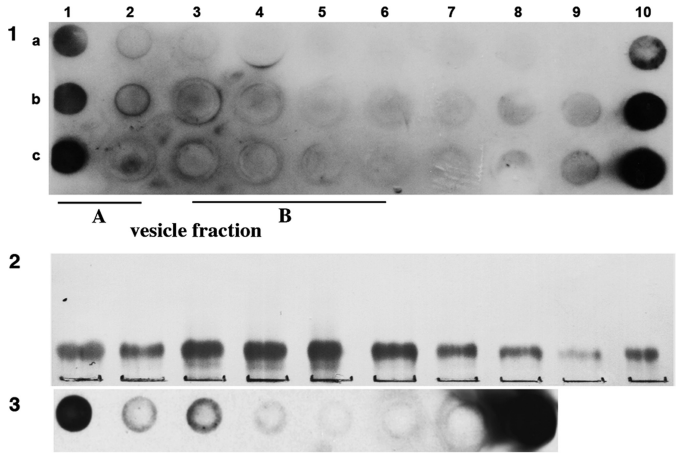

FIGURE 5. **Cholera toxin also binds a minor subfraction of GM1/cholesterol vesicles.** Cholera toxin was added above GM1/cholestrol vesicle constructs and vesicles separated on a discontinuous sucrose gradient. After separation, fractions (*1* (*top*)-*10*) were tested for cholera toxin content (*panel 1*). Cholera toxin binding is only found in fraction 1 (vesicle fraction A). GM1 extracted from gradient fractions was detected by CTxB TLC overlay (*panel 2*). GM1 is distributed in the gradient but accumulates in fractions 3, 4, 5, and 6 (vesicle fraction B). Anti-GM1 was included in a similar GM1/cholesterol vesicle gradient (*panel 3*) and immunodetected in the separated fractions.

Galactosyl or Glucosyl Ceramide Can "Expose" VT1 Undetectable Gb_3 in Fraction B Vesicles—To study how Gb_3 is rendered undetectable in fraction B vesicles, we incorporated other lipids within the Gb_3/cholesterol matrix. Most showed no effect, but galactosyl ceramide (non-hydroxy or hydroxy fatty acid form) "unmasked" fraction B vesicles for VT1 binding (Fig. 6*A*). Using a VT1 TLC overlay binding assay, Gb_3 was found to bind GalCer, GlcCer, and LacCer (Fig. 6*B*). LysoGalCer and adamantylGalCer were not bound, suggesting aglycone modulation (54). The binding of Gb_3 to GalCer may counter cholesterol masking of Gb_3 for VT1 in fraction B vesicles. GlcCer and LacCer were tested to unmask fraction B vesicles for VT1 binding (Fig. 6*C*), but only GlcCer was active.

VT1 Binding Cell-derived Gb_3 Vesicles: Resolution of Undetectable GSL—Vero cell post-nuclear supernatant membranes were extracted with Triton X-100 at 4 °C and subjected to VT1/sucrose-density gradient centrifugation at ambient temperature. As for the model GSL/cholesterol vesicles, VT1-bound vesicles were found only in a light fraction (vesicle fraction A; Fig. 7, *A* and *B*, *row a*), separate from the major GSL-containing fractions (vesicle fraction B; Fig. 7*A*, *panel d*). Vesicle fraction B also contained most phospholipids (Fig. 7*A*, *panel c*). For Gb_3-depleted DRM vesicles, from cells grown with the glucosyl ceramide synthase inhibitor, P4 (46), no VT1 binding was detected (Fig. 7*A*, *rows b* and *f*). Selective depletion of GSLs by P4 was confirmed by TLC of gradient fraction extracts (not shown). Caveolin, a cholesterol binding (55) DRM marker protein (56), accumulated together with GM1/Gb_3 in fractions 4 and 5. Lower levels were also in the VT1-bound fraction (Fig. 7*A*, *row g*).

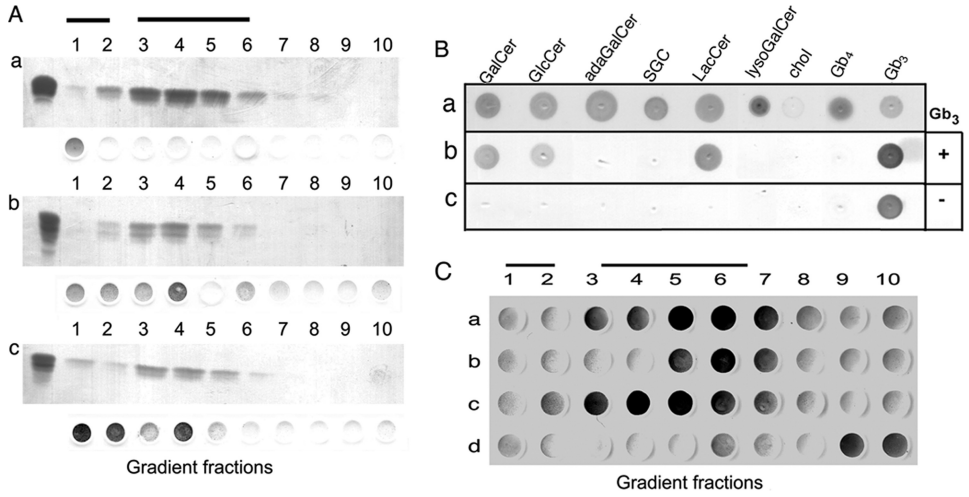

FIGURE 6. **Galactosyl or glucosyl ceramide can unmask Gb_3/cholesterol for VT1 binding, and bind Gb_3 directly.** *A*, Gb_3/cholesterol vesicles were separated in a VT1-containing sucrose gradient and vesicle-bound VT1 detected by immunoblot and compared with Gb_3 distribution. *Panels a–c*: *upper section*, VT1-TLC overlay to detect Gb_3 in GSL extract of gradient fractions: *left-most lane*, Gb_3 standard; *lower section*: immunodetection of vesicle-bound VT1 in gradient fractions. *a*, Gb_3/cholesterol vesicles; *b*, GalCer (non-hydroxy fatty acid)/Gb_3/cholesterol vesicles; *c*, GalCer (hydroxy fatty acid)/Gb_3/cholesterol vesicles. Vesicle fractions A and B are indicated as *bars* above the *panels*. *B*, GSLs were screened for Gb_3 binding. Purified lipids (GalCer, GlcCer, adamantyl-GalCer, SGC, LacCer, lysoGalCer, cholesterol, Gb_4, and Gb_3) were spotted on TLC and detected by orcinol (*a*). Similar plates were incubated ± "aqueous" Gb_3 and then tested for VT1 binding (*b* and *c*). *C*, GalCer, GlcCer, and LacCer were compared for effect on Gb_3/cholesterol vesicle binding in a VT1-containing sucrose gradient. Vesicle-bound VT1 was detected by immunoblot. *a*, GalCer (non-hydroxy fatty acid)Gb_3/cholesterol vesicles; *b*, GalCer (hydroxy fatty acid)/Gb_3/cholesterol vesicles; *c*, GlcCer/Gb_3/cholesterol vesicles; *d*, LacCer/Gb_3/cholesterol vesicles. Vesicle fractions A and B are indicated as *bars* above *panel C*.

Thus, the majority of the cellular Gb_3 in these membrane vesicles of complex lipid/protein composition (the standard "DRM" fraction), was "masked" from VT1 binding, and a lighter, VT1-reactive, minor Gb_3-containing fraction detected, in a manner similar to the model Gb_3/cholesterol vesicle system. This shows ligand-undetectable GSL is a property shared by cell-derived membranes. MβCD cholesterol extraction of cell-derived DRMs resulted in the loss of VT1 binding in fraction 2 (*i.e.* vesicle fraction A) and a gain of binding to fractions 4 and 5 (vesicle fraction B) (Fig. 7*B*, *row b*), indicating a key role for cholesterol in this aglycone reg-

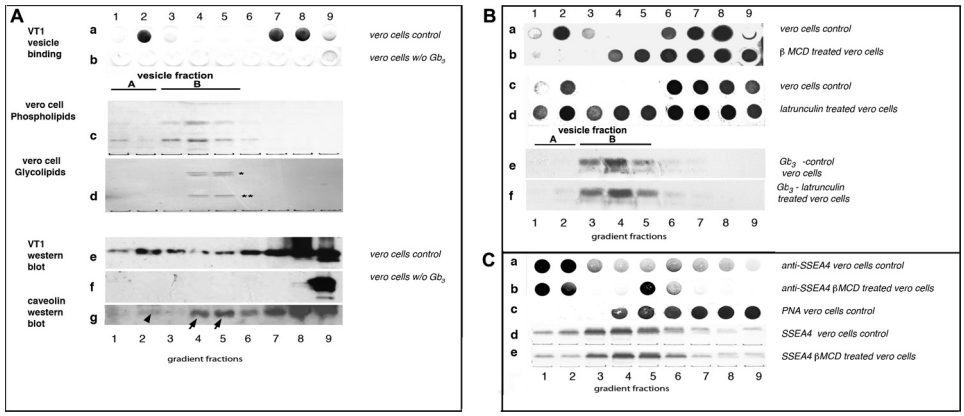

FIGURE 7. **Cell membrane-derived vesicles show similar, cholesterol dependent, minor ligand-bound, and major ligand-unbound GSL fractions.** The Triton extracts of cell membranes prepared from control Vero cells or cells grown in P4 to deplete Gb_3, were separated on a VT1 containing sucrose gradient. Control cell membranes were also extracted ± βMCD or treated ± latrunculin prior to detergent treatment. Vesicle-bound VT1 was detected in dot-blotted gradient fractions, and total VT1 by Western blot of gradient fractions. mAb anti-SSEA4 (globoseries embryonic GSL antigen) binding to gradient-separated Vero cell vesicles was assessed. In *A*: *a*, immunoblot detecting VT1 binding to control Vero cell membrane vesicles; *b*, VT1 binding to membrane vesicles from P4-treated (GSL-depleted) cells; *c*, phospholipids within the lipid extract of gradient fractions separated by TLC, were detected by iodine staining (*upper band*, PE; *lower*, PC); *d*, simultaneous detection of Gb_3 (*) and GM1 (**) distribution by VT1 and CTxB TLC overlay of the fractions shown in *c*; *e*, VT1 A subunit detection by Western blot of gradient fractions from control cell membranes (compare with *a*); *f*, anti-VT1 Western blot of gradient fractions of membranes from P4-treated cells (compare with *b*); *g*, anti-caveolin Western blot of control cell gradient fractions. *Arrows* indicate caveolin accumulation in the classic DRM fraction 5. Caveolin was also detected in the VT1-binding fraction 2 (*arrowhead*). In *B*: *a*, VT1 binding to control Vero cell membrane vesicles as in *A*, *panel a*; *b*, VT1 binding to vesicles from MβCD-treated Vero cell membranes; *c*, immunoblot detection of VT1 within the gradient, binding to control Vero cell DRM vesicles; *d*, VT1 binding to separated DRM vesicles from latrunculin-treated cells; *e*, VT1/TLC overlay to detect Gb_3 in GSL extract of control cell vesicle fractions; *f*, VT1/TLC overlay to detect Gb_3 in GSL extract of latrunculin-treated cell vesicle fractions. In *C*: *a*, anti-SSEA4 binding to gradient-separated control Vero cell DRM vesicles or (*b*) MβCD-treated Vero cell vesicles; *c*, peanut agglutinin lectin binding to gradient-separated DRM vesicles as used in *a*; GSLs were extracted from the gradient fractions, separated by TLC, and immunostained with anti-SSEA4; *d*, Vero cell gradient fraction GSLs; and *e*, MβCD-treated Vero cell gradient fraction GSLs.

ulation of cell membrane Gb_3 receptor function. Discordant Gb_3 receptor activity for VT1 was seen for Vero cell membrane vesicles prepared at 37 °C (57) or (though less well resolved) without detergent (58) (see supplemental Fig. 1). Inhibition of cell actin polymerization with latrunculin B before DRM preparation also induced the subsequent binding of VT1 within vesicle fraction B (Fig. 7*B*, *rows c* and *d*) without effect on Gb_3 distribution (Fig. 7*B*, *rows e* and *f*). Unlike cholesterol depletion (Fig. 7*B*, *row b*), latrunculin enhanced, rather than reduced, vesicle fraction A VT1 binding (Fig. 7*B*, *row d*).

mAb binding to SSEA-4, a globoseries GSL embryonic differentiation antigen (59), was similarly apparent only for Vero cell-derived vesicle fraction A (Fig. 7*C*, *row a*) containing only a minor fraction of the total SSEA4 (Fig. 7*C*, *row d*). Anti-SSEA4 fraction B vesicle binding was induced after cholesterol extraction of the vesicles (Fig. 7*C*, *row b*). Peanut agglutinin lectin bound to glycoproteins present in the high density fractions, including fraction B (Fig. 7*C*, *row c*), showing that cholesterol masking is a GSL-selective carbohydrate property.

The same discrepancy between ligand binding and GSL gradient distribution was observed when VT1 and CTx were bound together to Vero cells prior to DRM isolation (Fig. 8, *A* and *B*). The major VT1 and CTx binding fractions were at the top of the gradient (vesicle fraction A), separate from the bulk GSL-containing DRMs at the 5/30% sucrose interface (cell-derived vesicle fraction B) (Fig. 8*C*). Vero cell MβCD cholesterol depletion prior to toxin binding resulted in loss of vesicle fraction A binding and induction of vesicle fraction B binding of both VT1 and CTx. Cell treatment with cholesterol oxidase reduced vesicle fraction A binding but was less effective to unmask "invisible" cellular Gb_3 and GM1 (Fig. 8, *A* and B, *row b* compare with *row c*).

The Gb_3 fatty acid isoforms of Vero cell-derived fraction A and B were analyzed by HPLC/MS (supplemental Table 1). C24:0 and C24:1 are the major Gb_3 species in both fractions, although the C24:0/C24:1 ratio was lower in fraction B. The overall Gb_3 content of fraction A was 10% that of fraction B. Cholesterol extraction with MβCD did not significantly alter the Gb_3 fatty acid profile in each fraction.

Detection of Invisible Gb_3 on Intact Cells—Our studies predict two cell membrane GSL pools. These "ligand-available" and "cholesterol-masked" Gb_3 membrane pools were visualized on Vero and HeLa cells using differentially labeled VT1 B (Fig. 9). VT1-B surface binding of Vero cells retained a punctate domain distribution after cholesterol depletion (Fig. 9*A*). The ligand-available cell surface Gb_3 was internalized by warming the cells after Alexa488-VT1B binding, and the invisible Gb_3 was detected by subsequent cholesterol extraction then labeling at 4 °C with Texas Red-VT1B (Fig. 9, *B* and *C*). Within each cell, the amount of each Gb_3 pool did not necessarily correlate; cells with low or high ligand-available (*green*) Gb_3 could have a major or minor cholesterol-masked (*red*) Gb_3 pool.

DISCUSSION

A model membrane system was developed (42) to study whether variability of GSL receptor function according to lipid structure/microenvironment (aglycone) modulation and the accumulation of GSLs within cholesterol-enriched microdomains were linked. The ~1:1 GSL:cholesterol molar ratio optimized VT1-Gb_3 binding, but similar ratios are found in some natural membranes (60). By density gradient equilibrium centrifugation, we have separated a ligand binding, minor GSL/cholesterol vesicle population from the major vesicle population not recognized by most GSL-binding proteins. This novel invisible GSL/cholesterol format surprisingly predicted a property of cell membranes: the major fraction of cellular GSLs is prevented from protein binding, largely by cholesterol masking.

Undetectable Model Membrane GSLs—Only 5–10% the total GSL within our model GSL/cholesterol vesicles (fraction A), could bind ligands (VT1,VT2, gp120, lectin, CTxB, or anti-GSL antibodies). The vesicle fraction B (at the 5–30% sucrose interface) contains 90% of the GSL but is refractory to ligand binding

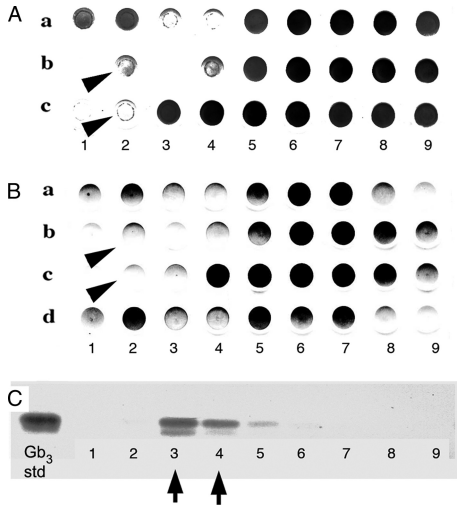

FIGURE 8. **VT1 and CTx bind only a minor fraction of cell plasma membrane Gb_3 and GM1.** Vero cells were co-incubated with VT1 and CTx. Some cells were treated with cholesterol oxidase or MβCD for 1 h prior to toxin addition. Cells were then extracted with Triton, and the extracts were separated on a sucrose gradient (fractions 1–9). Toxin distribution within the gradient was determined by immunoblot. *A*, VT1 distribution; *B*, CTx distribution: *lane a*, toxin bound at 23 °C for 30 min with no cell pretreatment; *lane b*, after cholesterol oxidase treatment; *lane c*, after MβCD treatment; *lane d*, CTx bound to cell DRMs after extraction. *C*, detection of Gb_3 in GSL extract of control Vero cell DRM fractions by VT1/TLC overlay. Cell-bound VT1/CTx separates as fraction 2 in the gradient (*i.e.* vesicle fraction A). This binding is eliminated for DRMs from cholesterol oxidase or MβCD-treated cells (*A* and *B*, *arrowheads*), but MβCD treatment induces vesicle fraction B VT1/CTx binding.

(invisible GSL). Although much of the GSL is unavailable due to multilamellar structure, the binding of mAb IgM anti-Gb_3 to vesicle fraction B, both by vesicle immunostaining and to the outer membrane leaflet by IEM, shows the Gb_3 of these vesicles is surface-available. Because this property was shared by seven protein ligands and four receptor GSLs (Gb_3, GalCer, SGC, and GM1), this could be a general GSL effect. IgM mAb anti-Gb_3 binding to both vesicle fraction A (preferentially) and vesicle fraction B suggests a carbohydrate conformation change may mask Gb_3 in vesicle fraction B. Molecular simulation predicts such a cholesterol-mediated change (61).[3]

A difference between the Gb_3 carbohydrate hydroxyl groups required for IgM mAb anti-Gb_3 and VT1/VT2 Gb_3 binding (20) involved hydroxyl groups which restricted rotation around the glycosidic linkages. If cholesterol restricts rotation around these glycosidic bonds within vesicle fraction B, a selective effect on VT1/VT2 compared with IgM mAb anti-Gb_3 binding might result. Thus GSL mobility in these vesicles may be necessary for (most) ligand binding. The fatty acid dependence of ligand-Gb_3 binding for fraction A vesicles led to a similar conclusion (19). Hydrogen bonds between cholesterol and sphingolipids (63) may restrict GSL motion.

Gradient resolution, promoted by reduced tube size (see supplemental material) permitted complete separation of ligand-detectable and -invisible GSL/cholesterol vesicles. Without detergent, Gb_3 accumulates mainly in the denser gradient fractions. Solubilizing weaker interactions results in separation of two vesicular fractions, in only the minor of which is the GSL

[3] D. Lingwood, B. Binnington, T. Róg, I. Vattulainen, M. Grzybek, U. Coskun, C. Lingwood, and K. Simons, submitted for publication.

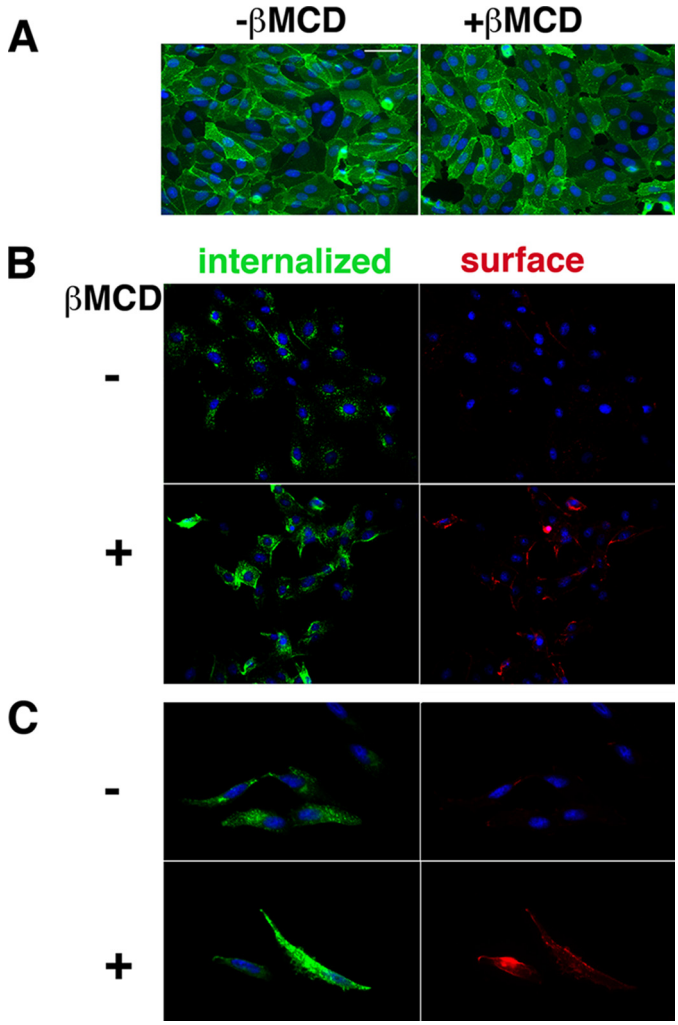

FIGURE 9. **Detection of two cell surface GSL pools; unmasking invisible Gb_3 by cholesterol depletion.** *A*, Alexa488-VT1B binding to Vero cells at 4 °C prior to or after MβCD cholesterol depletion. VT1B punctate surface binding distribution is retained. *B*, Vero cells or (*C*) HeLa cells were labeled with Alexa488-VT1B and warmed at 37 °C for 15 min to internalize bound VT1B. Cells were incubated ± MβCD as indicated at 37 °C then chilled on ice and re-labeled with Texas Red-VT1B to detect newly available pools of Gb_3. *Bar* = 400 nm. DAPI nuclear staining is *blue*.

available for ligand binding. Detergent as a tool in cell biology has been criticized (64), largely in relation to the often overextrapolated connection between membrane detergent insolubility and the cellular existence of the nanoscale sphingolipid-cholesterol-related membrane heterogeneity of lipid rafts (25, 65). Although detergent-resistant membranes do not reflect the native membrane organization, insolubility can reflect specific cellular lipid and protein interactions (57).

Two Cell Membrane GSL Pools—The principle defined with our simple GSL/cholesterol membrane model, that GSL bilayers have a major fraction unavailable for ligand binding, is largely recapitulated within cell plasma membrane vesicles, and cells themselves. The VT1 binding fraction within the Vero cell DRMs (vesicle fraction A) was separated from the bulk Gb_3-containing vesicle fraction, at the 5/30% sucrose interface, as for the model vesicle constructs. The DRM markers, GM1 and caveolin, also identified this cell-derived vesicle fraction B. Caveolin is also in vesicle fraction A. The bulk Gb_3 (and GM1)-

containing fraction B, unbound by VT1 (or CTx), shows that invisible GSL vesicles are readily prepared from cell membranes. Because this discord in GSL receptor activity was seen for vesicles prepared from VT1/CTx-treated cells, most plasma membrane Gb_3/GM1 is also invisible.

Cholesterol depletion of Vero cell membrane DRMs after preparation, and Vero cells prior to extraction, resulted in the same loss of VT1 (and CTx) binding to vesicle fraction A and the induction of VT1/CTx binding to vesicle fraction B. Thus, cholesterol is central in cell membrane GSL masking. Cholesterol masking of GM1 may compromize CTx as a lipid raft marker. Some cholesterol is required for optimal ligand binding (vesicle fraction A) but cholesterol can also prevent GSL recognition (vesicle fraction B). VT1 binding in higher density cell membrane fractions near the bottom of the gradient is Gb_3-dependent and may represent unresolved and detergent-soluble Gb_3. Differential Gb_3 fatty acid content did not explain the differential fraction A *versus* B ligand binding or the effect of cholesterol depletion (supplemental material).

Unmasking Invisible Membrane Gb_3—Although cholesterol depletion increased ligand binding in cell membrane vesicle fraction B, the GSL content of fraction B was unaltered. Cholesterol depletion of cell membranes did not render ligand binding to fraction B vesicles proportional to GSL content, indicating other components restrict fraction B GSL receptor function. Although the mechanism of cholesterol-GSL masking is not yet defined, our finding that inclusion of GalCer or GlcCer in the model vesicles can reverse cholesterol-Gb_3 masking provides a probe. Gb_3 binding GalCer, GlcCer, and LacCer may be new examples of GSL carbohydrate-carbohydrate interaction (54). In the novel VT1-TLC overlay assay devised to screen for GSL-GSL binding, the aqueous Gb_3 sample likely contains micelles, and therefore it is unclear as yet, whether VT1 can bind Gb_3 bound to another GSL. Although no Gb_3-cholesterol binding was seen, hydrophobic interactions may still play a significant role. These monohexosides may counter aglycone masking of membrane Gb_3 receptor function. GalCer/GlcCer-Gb_3 binding in fraction B vesicles may cluster Gb_3, or increase fluidity to allow multivalent VT1 binding (9). Gb_3 bound to LacCer may be too large or immobile to promote VT1 fraction B vesicle binding. Reduced GlcCer levels can decrease VT1 binding to cell DRMs (34), which may be a function of the GlcCer/GalCer-Gb_3 binding and unmasking we observe. Interestingly, intracellular Gb_3-dependent VT1 trafficking was found to be selectively dependent on C16 ceramide monohexoside (66).

Cell Physiology of Invisible GSL—Disruption of the cellular actin cytoskeleton in cells with latrunculin also resulted in partial unmasking of invisible cell membrane Gb_3 for VT1 binding. VT1 binding to fraction A vesicles was also increased (unlike cholesterol depletion), consistent with a cytoskeleton-lipid microdomain interaction (67, 68). A cholesterol-cytoskeletal linkage (69) might alter GSL receptor function during dynamic cell membrane-remodeling processes. Cholesterol is increased at the motile cell membrane leading edge (70) and is required (71) and selectively regulated (72, 73) during mitosis. Cholesterol synthesis inhibitors induce stem cell differentiation and anchorage-dependent tumor cell growth (74). The differential distribution of cholesterol in cellular membranes (75–77), its potential asymmetric cell surface topology (78, 79), and accumulation in GSL enriched rafts could provide extensive dynamic lateral regulation of GSL function. Such domains play many (patho)physiological roles, *e.g.* in signal transduction (80) and microbial pathogenesis (81, 82). GSL masking could be central to such processes and provide new bases for prophylaxis of GSL-targeted infectious disease.

SSEA-4 (stage-specific embryonic antigen 4) is a globoseries GSL (NeuAcα2–3Galβ1–3GalNAcβ1–3Galα1–4Galβ1–4Glc ceramide (83)), the major marker defining human pluripotent stem cells (84). Antibody/SSEA-4 binding is key in immuno-sorting undifferentiated cells (85) for potential therapeutic uses. Cholesterol masking SSEA-4 in fraction B Vero cell vesicles so only 10% of cell membrane SSEA-4 is available for antibody binding suggests practical relevance of invisible membrane GSL. The greater polarity of SSEA-4 ganglioside indicates cholesterol-GSL masking is independent of GSL headgroup character. Because peanut agglutinin bound glycoproteins in cellular fraction B vesicles, cholesterol masking is restricted to GSL cell glycoconjugates.

Cholesterol depletion of Vero cells unmasked invisible Gb_3 to allow distinct VT1B cell staining. The two separate cell membrane Gb_3 pools (ligand-available and cholesterol-masked) were clearly delineated by differential VT1B labeling. The non-uniform surface distribution of the (initially) invisible Gb_3 pool, consistent with retention in lipid rafts (86), its relation to the initial, ligand-bound Gb_3, and defining other factors, which restrict cell membrane GSL recognition, will provide a new arena for membrane GSL receptor studies. The topical separation of these pools implies separate regulation.

Several studies already indicate a physiological role for membrane GSL masking by cholesterol. Cholesterol depletion can unmask Gb_3 in human renal glomeruli (20, 28). Strong, detergent-resistant VT1/VT2 binding was induced in VT1/VT2 unreactive glomeruli after cholesterol extraction. Thus membrane cholesterol masking of Gb_3 may protect against VT-induced glomerular pathology and provide a risk factor for VT-induced hemolytic uremic syndrome. Cholesterol depletion to unmask membrane GSLs is also a key feature of capacitation of spermatozoa required for fertility (87, 88). The standard use of acetone (extracts steroids) to "unmask" GSLs for immunohistochemistry (89, 90) further attests to widespread cholesterol membrane GSL masking in cells and tissues.

Molecular modeling the cholesterol-sphingolipid complex shows the polar cholesterol hydroxyl group (63), can form an H-bond network to alter the sugar conformation around the anomeric linkage, to be parallel, rather than perpendicular, to the membrane (61). We have found similar simulation results for GM1 ganglioside.[3] Thus, membrane cholesterol could alter GSL carbohydrate conformation, a potential on/off switch for protein recognition. This aglycone modulation translates "cis" interactions into "trans" effects. This could be bidirectional. Protein binding to membrane-available GSL might alter lateral bilayer interactions (86).

The GSL:cholesterol ratio was constant in model vesicle fractions A and B. The interaction of cholesterol with sphingolipids is more pronounced than glycerolipids, but both vary with acyl chain length (C16 → C20) and saturation (91). Within Gb_3/cholesterol vesicle fraction A, receptor activity for VT1 and gp120 is a function of the Gb_3 fatty acid chain length in this range. From Gb_3 fatty acid isoform mixing, we proposed that reduced Gb_3 fluidity could restrict ligand binding to vesicle fraction A (19). Membrane parallel GSL carbohydrate would be expected to reduce fluidity. Fluidity could also provide a basis for the differential ligand binding to vesicle fractions A and B. The major difference between vesicle fractions A and B is size. Increased membrane curvature can increase model membrane lipid headgroup fluidity (92) and promote ligand binding (93). Decreased Gb_3 fluidity in fraction B vesicles could restrict clustering of GSL necessary for multivalent ligand binding (9).

GSL carbohydrate conformation (10, 94) is also restricted by the plane of the membrane (11). Membrane curvature may alter the plane of the membrane bilayer relative to the GSL carbohydrate (29, 61) to affect ligand binding. GSL carbohydrate conformation may also affect membrane curvature and vesicle size. The gradient separation of cellular VT1-bound Gb_3 and CTx-bound GM1 membranes from the bulk GSL-containing fraction suggests these domains are physically separate in cells, for example, binding ligand in areas of high membrane curvature (95).

Uncertain Detection—In our model vesicles, high levels of Gb_3 (or other GSLs) are undetectable. If as physiologically relevant as our cell-derived vesicles indicate, an "uncertainty principle" for molecular distribution of GSLs in cells should be considered. Undetectable membrane GSLs raise questions concerning asymmetric GSL distribution in cell and tissue membranes. GSLs are considered present only on the outer plasma membrane leaflet and inner leaflet of cellular organelles. Phospholipids can flip between leaflets, and the asymmetric plasma membrane aminophospholipid bilayer distribution is maintained by an energy-dependent translocase, an early casualty of apoptosis (96). Short sugar chain GSLs are no more polar than phospholipids (indeed PC is more polar than Gb_3) and should flip to equilibrate across a membrane bilayer at rates comparable to phospholipids. However, no translocase for GSLs has been reported to reverse this tendency. Why then should GSL asymmetry, defined by synthesis, be maintained at the cell surface (or elsewhere)? Such asymmetry has been defined empirically by ligand (antibody, enzyme, toxin, and lectin) binding, but our studies now show absence of ligand binding may not necessarily indicate absence of membrane GSL. Although this is counter to current cell membrane paradigms, some studies have implied the presence of GSLs on the cytosolic membrane surface (62).

A remarkable discrepancy in GSL receptor function, defined in simple GSL/cholesterol vesicles, describes a new thermodynamic property of hyper- *versus* hypo-cell membrane GSL receptor activity, which may apply generally, *i.e.* cholesterol (in part) prevention of ligand recognition of the major cellular GSL fraction. This intrinsic lipid bilayer property may be modulated by other membrane components, such as the actin cytoskeleton, to make aglycone GSL masking a potential dynamic "cloaking device" in cellular physiology.

Acknowledgments—We thank Dr. L. Kyriakopoulou, Dept. of Pediatric Laboratory Medicine, Hospital for Sick Children, for Gb_3 mass spectrometry and Dr. D. Lingwood, MPI.CPG Max Planck Inst., Dresden, for helpful discussion.

REFERENCES

1. Lingwood, C. A. (1996) *Glycoconj. J.* **13,** 495–503
2. Ackerman, G. A., Wolken, K. W., and Gelder, F. B. (1980) *J. Histochem. Cytochem.* **28,** 1334–1342
3. Hakomori, S. (1981) *Annu. Rev. Biochem.* **50,** 733–764
4. Nakakuma, H., Horikawa, K., Kawaguchi, T., Hidaka, M., Nagakura, S., Hirai, S., Kageshita, T., Ono, T., Kagimoto, T., Iwamori, M., *et al.* (1992) *Jpn. J. Clin. Oncol.* **22,** 308–312
5. Kannagi, R., Stroup, R., Cochran, N. A., Urdal, D. L., Young, W. W., Jr., and Hakomori, S. I. (1983) *Cancer Res.* **43,** 4997–5005
6. Crook, S. J., Boggs, J. M., Vistnes, A. I., and Koshy, K. M. (1986) *Biochemistry* **25,** 7488–7494
7. Nakakuma, H., Ari, M., Kawaguchi, T., Horikawa, K., Hidaka, M., Sakamoto, K., Iwamori, M., Nagai, Y., and Takatsuki, K. (1989) *FEBS Lett.* **258,** 230–232
8. Römer, W., Berland, L., Chambon, V., Gaus, K., Windschiegl, B., Tenza, D., Aly, M. R., Fraisier, V., Florent, J. C., Perrais, D., Lamaze, C., Raposo, G., Steinem, C., Sens, P., Bassereau, P., and Johannes, L. (2007) *Nature* **450,** 670–675
9. Windschiegl, B., Orth, A., Römer, W., Berland, L., Stechmann, B., Bassereau, P., Johannes, L., and Steinem, C. (2009) *PLoS One* **4,** e6238
10. Nyholm, P. G., and Pascher, I. (1993) *Int. J. Biol. Macromol.* **15,** 43–51
11. Strömberg, N., Nyholm, P. G., Pascher, I., and Normark, S. (1991) *Proc. Natl. Acad. Sci. U.S.A.* **88,** 9340–9344
12. Stewart, R. J., and Boggs, J. M. (1993) *Biochemistry* **32,** 5605–5614
13. Boyd, B., Magnusson, G., Zhiuyan, Z., and Lingwood, C. A. (1994) *Eur. J. Biochem.* **223,** 873–878
14. Mamelak, D., Mylvaganam, M., Whetstone, H., Hartmann, E., Lennarz, W., Wyrick, P., Raulston, J., Han, H., Hoffman, P., and Lingwood, C. A. (2001) *Biochemistry* **40,** 3572–3582
15. Strömberg, N., and Karlsson, K. A. (1990) *J. Biol. Chem.* **265,** 11244–11250
16. Angström, J., Teneberg, S., Milh, M. A., Larsson, T., Leonardsson, I., Olsson, B. M., Halvarsson, M. O., Danielsson, D., Näslund, I., Ljungh, A., Wadström, T., and Karlsson, K. A. (1998) *Glycobiology* **8,** 297–309
17. Kiarash, A., Boyd, B., and Lingwood, C. A. (1994) *J. Biol. Chem.* **269,** 11138–11146
18. Binnington, B., Lingwood, D., Nutikka, A., and Lingwood, C. A. (2002) *Neurochem. Res.* **27,** 807–813
19. Mahfoud, R., Manis, A., and Lingwood, C. A. (2009) *J. Lipid Res.* **50,** 1744–1755
20. Hinoi, E., Takarada, T., Ueshima, T., Tsuchihashi, Y., and Yoneda, Y. (2004) *Eur. J. Biochem.* **271,** 1–13
21. Tam, P., Mahfoud, R., Nutikka, A., Khine, A. A., Binnington, B., Paroutis, P., and Lingwood, C. (2008) *J. Cell. Physiol.* **216,** 750–763
22. Brown, D. A., and London, E. (2000) *J. Biol. Chem.* **275,** 17221–17224
23. Lundén, B. M., Löfgren, H., and Pascher, I. (1977) *Chem Phys Lipids* **20,** 263–271
24. Mylvaganam, M., and Lingwood, C. A. (2003) in *Carbohydrate-based Drug Discovery* (Wong, C. H., ed) pp. 761–780, Wiley-VCH Press, Weinheim, Germany
25. Brown, D. A. (2006) *Physiology* **21,** 430–439
26. Lingwood, D., and Simons, K. (2010) *Science* **327,** 46–50
27. Helenius, A., and Simons, K. (1975) *Biochim. Biophys. Acta* **415,** 29–79
28. Khan, F., Proulx, F., and Lingwood, C. A. (2009) *Kidney Int.* **75,** 1209–1216
29. Lingwood, C. A., Manis, A., Mahfoud, R., Khan, F., Binnington, B., and Mylvaganam, M. (2010) *Chem. Phys. Lipids* **163,** 27–35
30. Lingwood, C. A. (1999) *Biochim. Biophys. Acta* **1455,** 375–386
31. Okuda, T., Tokuda, N., Numata, S., Ito, M., Ohta, M., Kawamura, K.,

Wiels, J., Urano, T., Tajima, O., and Furukawa, K. (2006) *J. Biol. Chem.* **281,** 10230–10235
32. Katagiri, Y. U., Mori, T., Nakajima, H., Katagiri, C., Taguchi, T., Takeda, T., Kiyokawa, N., and Fujimoto, J. (1999) *J. Biol. Chem.* **274,** 35278–35282
33. Falguières, T., Mallard, F., Baron, C., Hanau, D., Lingwood, C., Goud, B., Salamero, J., and Johannes, L. (2001) *Mol. Biol. Cell* **12,** 2453–2468
34. Smith, D. C., Sillence, D. J., Falguières, T., Jarvis, R. M., Johannes, L., Lord, J. M., Platt, F. M., and Roberts, L. M. (2006) *Mol. Biol. Cell* **17,** 1375–1387
35. Bhat, S., Spitalinik, S. L., Gonzalez-Scarano, F., and Silberberg, D. H. (1991) *Proc. Natl. Acad. Sci.* **88,** 7131–7134
36. Mylvaganam, M., and Lingwood, C. A. (1999) *J. Biol. Chem.* **274,** 20725–20732
37. Villard, R., Hammache, D., Delapierre, G., Fotiadu, F., Buono, G., and Fantini, J. (2002) *Chembiochem* **3,** 517–525
38. Liao, Z., Cimakasky, L. M., Hampton, R., Nguyen, D. H., and Hildreth, J. E. (2001) *AIDS Res. Hum. Retroviruses* **17,** 1009–1019
39. Viard, M., Parolini, I., Sargiacomo, M., Fecchi, K., Ramoni, C., Ablan, S., Ruscetti, F. W., Wang, J. M., and Blumenthal, R. (2002) *J. Virol.* **76,** 11584–11595
40. Lund, N., Branch, D., Mylvaganam, M., Chark, D., Ma, X., Sakac, D., Binnington, B., Fantini, J., Puri, A., Blumenthal, R., and Lingwood, C. (2006) *AIDS* **20,** 333–343
41. Lund, N., Olsson, M. L., Ramkumar, S., Sakac, D., Yahalom, Y., Levene, C., Hellberg, A., Ma, X. Z., Jung, D., Binnington, B., Lingwood, C. A., and Branch, D. R. (2009) *Blood* **113,** 4980–4991
42. Nutikka, A., and Lingwood, C. (2004) *Glycoconj. J.* **20,** 33–38
43. Nutikka, A., Binnington-Boyd, B., and Lingwood, C. A. (2003) in *Methods in Molecular Medicine* (Philpot, D., and Ebel, F., eds) pp. 187–195, Humana Press, Totowa, NY
44. Pellizzari, A., Pang, H., and Lingwood, C. A. (1992) *Biochemistry* **31,** 1363–1370
45. Wiels, J., Fellous, M., and Tursz, T. (1981) *Proc. Nat. Acad. Sci. U.S.A.* **78,** 6485–6488
46. Lee, L., Abe, A., and Shayman, J. A. (1999) *J. Biol. Chem.* **274,** 14662–14669
47. Tam, P., and Lingwood, C. A. (2007) *Microbiology* **153,** 2700–2710
48. Abramoff, M. D., Magelhaes, P. J., and Ram, S. J. (2004) *Biophotonics Int.* **11,** 36–42
49. Fantini, J., Cook, D. G., Nathanson, N., Spitalnik, S. L., and Gonzalez-Scarano, F. (1993) *Proc. Natl. Acad. Sci. U.S.A.* **90,** 2700–2704
50. Lowry, R. R. (1968) *J. Lipid Res.* **9,** 397
51. Nutikka, A., Binnington-Boyd, B., and Lingwood, C. (2003) in *Methods in Molecular Medicine* (Philpot, D., and Ebel, F., eds) pp. 197–208, Humana Press, Totowa, NY
52. Hirai, M., Koizumi, M., Hirai, H., Hayakawa, T., Yuyama, K., Suzuki, N., and Kasahara, K. (2005) *J. Phys. Condens. Matter* **17,** S2965–S2977
53. Hammache, D., Yahi, N., Maresca, M., Piéroni, G., and Fantini, J. (1999) *J. Virol.* **73,** 5244–5248
54. Hakomori, S. (2004) *Arch. Biochem. Biophys.* **426,** 173–181
55. Murata, M., Peränen, J., Schreiner, R., Wieland, F., Kurzchalia, T. V., and Simons, K. (1995) *Proc. Natl. Acad. Sci. U.S.A.* **92,** 10339–10343
56. Czarny, M., Lavie, Y., Fiucci, G., and Liscovitch, M. (1999) *J. Biol. Chem.* **274,** 2717–2724
57. Chen, X., Jen, A., Warley, A., Lawrence, M. J., Quinn, P. J., and Morris, R. J. (2009) *Biochem. J.* **417,** 525–533
58. Macdonald, J. L., and Pike, L. J. (2005) *J. Lipid Res.* **46,** 1061–1067
59. Sato, B., Katagiri, Y. U., Miyado, K., Akutsu, H., Miyagawa, Y., Horiuchi, Y., Nakajima, H., Okita, H., Umezawa, A., Hata, J., Fujimoto, J., Toshimori, K., and Kiyokawa, N. (2007) *Biochem. Biophys. Res. Commun.* **364,** 838–843
60. Di Biase, A., Salvati, S., and Serlupi Crescenzi, G. (1990) *Neurochem. Res.* **15,** 519–522
61. Yahi, N., Aulas, A., and Fantini, J. (2010) *PLoS One* **5,** e9079
62. Delacour, D., Gouyer, V., Zanetta, J. P., Drobecq, H., Leteurtre, E., Grard, G., Moreau-Hannedouche, O., Maes, E., Pons, A., André, S., Le Bivic, A., Gabius, H. J., Manninen, A., Simons, K., and Huet, G. (2005) *J. Cell Biol.* **169,** 491–501
63. Róg, T., and Pasenkiewicz-Gierula, M. (2006) *Biophys. J.* **91,** 3756–3767
64. Lingwood, D., and Simons, K. (2007) *Nat. Protoc.* **2,** 2159–2165
65. Hancock, J. F. (2006) *Nat. Rev. Mol. Cell Biol.* **7,** 456–462
66. Raa, H., Grimmer, S., Schwudke, D., Bergan, J., Wälchli, S., Skotland, T., Shevchenko, A., and Sandvig, K. (2009) *Traffic* **10,** 868–882
67. Lenne, P. F., Wawrezinieck, L., Conchonaud, F., Wurtz, O., Boned, A., Guo, X. J., Rigneault, H., He, H. T., and Marguet, D. (2006) *EMBO J.* **25,** 3245–3256
68. Chichili, G. R., and Rodgers, W. (2007) *J. Biol. Chem.* **282,** 36682–36691
69. Sun, M., Northup, N., Marga, F., Huber, T., Byfield, F. J., Levitan, I., and Forgacs, G. (2007) *J. Cell Sci.* **120,** 2223–2231
70. Mañes, S., and Martínez-A., C. (2004) *Trends Cell Biol.* **14,** 275–278
71. Fernández, C., Lobo Md Mdel, V., Gómez-Coronado, D., and Lasunción, M. A. (2004) *Exp. Cell Res.* **300,** 109–120
72. Bartz, R., Sun, L. P., Bisel, B., Wei, J. H., and Seemann, J. (2008) *EMBO J.* **27,** 948–955
73. Bengoechea-Alonso, M. T., Punga, T., and Ericsson, J. (2005) *Proc. Natl. Acad. Sci. U.S.A.* **102,** 11681–11686
74. Bracha, A. L., Ramanathan, A., Huang, S., Ingber, D. E., and Schreiber, S. L. (2010) *Nat. Chem. Biol.* **6,** 202–204
75. Orci, L., Montesano, R., Meda, P., Malaisse-Lagae, F., Brown, D., Perrelet, A., and Vassalli, P. (1981) *Proc. Natl. Acad. Sci. U.S.A.* **78,** 293–297
76. Bretscher, M. S., and Munro, S. (1993) *Science* **261,** 1280–1281
77. Lippincott-Schwartz, J., and Phair, R. D. (2010) *Annu. Rev. Biophys.* **39,** 559–578
78. Sato, S. B., Ishii, K., Makino, A., Iwabuchi, K., Yamaji-Hasegawa, A., Senoh, Y., Nagaoka, I., Sakuraba, H., and Kobayashi, T. (2004) *J. Biol. Chem.* **279,** 23790–23796
79. Hekman, M., Albert, S., Galmiche, A., Rennefahrt, U. E., Fueller, J., Fischer, A., Puehringer, D., Wiese, S., and Rapp, U. R. (2006) *J. Biol. Chem.* **281,** 17321–17336
80. Fielding, C. J., and Fielding, P. E. (2004) *Biochem. Soc. Trans.* **32,** 65–69
81. Goluszko, P., and Nowicki, B. (2005) *Infect. Immun.* **73,** 7791–7796
82. Heung, L. J., Luberto, C., and Del Poeta, M. (2006) *Infect. Immun.* **74,** 28–39
83. Kannagi, R., Cochran, N. A., Ishigami, F., Hakomori, S., Andrews, P. W., Knowles, B. B., and Solter, D. (1983) *EMBO J.* **2,** 2355–2361
84. Gang, E. J., Bosnakovski, D., Figueiredo, C. A., Visser, J. W., and Perlingeiro, R. C. (2007) *Blood* **109,** 1743–1751
85. Fong, C. Y., Peh, G. S., Gauthaman, K., and Bongso, A. (2009) *Stem Cell Rev.* **5,** 72–80
86. Jarvis, R. M., Chamba, A., Holder, M. J., Challa, A., Smith, D. C., Hodgkin, M. N., Lord, J. M., and Gordon, J. (2007) *Biochem. Biophys. Res. Commun.* **355,** 944–949
87. Kawano, N., Yoshida, K., Iwamoto, T., and Yoshida, M. (2008) *Biol. Reprod.* **79,** 1153–1159
88. Nixon, B., Bielanowicz, A., McLaughlin, E. A., Tanphaichitr, N., Ensslin, M. A., and Aitken, R. J. (2009) *J. Cell. Physiol.* **218,** 122–134
89. Kolling, G. L., Obata, F., Gross, L. K., and Obrig, T. G. (2008) *Histochem. Cell Biol.* **130,** 157–164
90. Sakumoto, Y., Ueta, H., Yuki, N., and Matsuno, K. (2009) *Arch. Histol. Cytol.* **72,** 77–90
91. McMullen, T. P., Lewis, R. N., and McElhaney, R. N. (1993) *Biochemistry* **32,** 516–522
92. Hutterer, R., Schneider, F. W., Pérez, N., Ruf, H., and Hof, M. (1993) *J. Fluorescence* **3,** 257–259
93. Iwamoto, K., Hayakawa, T., Murate, M., Makino, A., Ito, K., Fujisawa, T., and Kobayashi, T. (2007) *Biophys. J.* **93,** 1608–1619
94. Nyholm, P. G., and Pascher, I. (1993) *Biochemistry* **32,** 1225–1234
95. Hägerstrand, H., Mrówczyńska, L., Salzer, U., Prohaska, R., Michelsen, K. A., Kralj-Iglic, V., and Iglic, A. (2006) *Mol. Membr Biol.* **23,** 277–288
96. Das, P., Estephan, R., and Banerjee, P. (2003) *Life Sci.* **72,** 2617–2627